processes

MDPI

Article

Research on Properties of Ash and Slag Composite Cementitious Materials for Biomass Power Plants

Yanru Zhang [1], Baofeng Zhao [2], Jianjun Zhu [1], Zhenjiang Wang [1], Changzai Ren [2,*], Hongzhang Xie [2], Haibin Guan [2] and Di Zhu [2,*]

[1] National Energy Biomass Power Generation Group Co., Ltd., Beijing 100083, China
[2] Energy Research Institute, Qilu University of Technology (Shandong Academy of Sciences), Jinan 250014, China
* Correspondence: rcz@qlu.edu.cn (C.R.); zhud@sderi.cn (D.Z.)

Abstract: The effects of ash and slag from a biomass power plant on the compressive strength, setting time and fluidity of the pastes of Portland cement (P.O) and sulfoaluminate cement (SAC) were studied, and the hydration products and microstructure at the age of 7 days were analyzed via XRD, SEM and other test methods. The results show that the compressive strength of the composite cementitious material decreases, the setting time prolongs and the fluidity increases with the increase in the ash and slag content in the power plant. The microscopic analysis shows that the ash and slag of the biomass power plant can promote the hydration of Portland cement and sulfoaluminate cement paste, and increase the generation of hydration products. The results showed that replacing SAC clinker with 20–30% biomass power plant ash (BPPA) decreased the cement strength, and that an appropriate amount of BPPA (10–15%) could significantly improve the mechanical strength of SAC blended cement. The compressive strength of blended BPPA composite cementitious material in 28 days could reach 60 MPa. This study provided solutions to utilizing the BPPA as a building material admixture to minimize the consumption of energy-intensive cement and to meet the growing needs of the construction industry.

Keywords: biomass power plant ash and slag; Portland cement; calcium sulfoaluminate cement; mechanical properties; microstructure; hydration product

Citation: Zhang, Y.; Zhao, B.; Zhu, J.; Wang, Z.; Ren, C.; Xie, H.; Guan, H.; Zhu, D. Research on Properties of Ash and Slag Composite Cementitious Materials for Biomass Power Plants. *Processes* **2023**, *11*, 1627. https://doi.org/10.3390/pr11061627

Academic Editor: Young-Cheol Chang

Received: 14 April 2023
Revised: 18 May 2023
Accepted: 23 May 2023
Published: 26 May 2023

1. Introduction

With the annual expansion of the installed capacity of biomass power plants in China, the output of biomass power plant ash and slag is also experiencing annual growth. According to statistics, biomass power plants in China produce about 40 million tons of ash and slag per year [1]. The great accumulation of biomass power plant ash and slag due to the lack of effective ash and slag utilization technology has resulted in serious environmental problems (soil, water and air pollution). In the construction of a resource-saving, environmentally friendly society and a beautiful China, it is urgent to determine how to achieve the rapid and economic disposal of biomass power plant ash and slag and realize its harmlessness, reduction, and resource utilization.

Cement is the most widely used building material, the production of which consumes a lot of raw materials and energy and releases a great quantity of greenhouse gases. According to statistics, in 2020, China's cement output was 2.377 billion tons (about 55% of the world's total) and the CO_2 emissions in the corresponding production process reached 1.230 billion tons (about 12.1% of China's total carbon emissions) [2]. In the context of carbon peaking and carbon neutrality goals being a national strategy, carbon emission reduction in the construction industry, one of the industries related to carbon emissions, is expected to effectively drive the reduction in China's carbon emission peak by 2030, and help achieve half of China's carbon emission reduction targets by 2050 [3]. Therefore, a crucial step towards sustainable development in the country is a low-carbon development

route for the construction industry. To this end, replacing cement clinker with solid waste to prepare composite cementitious materials becomes a major approach to the sustainable development of the cement production industry. It can help reduce the greenhouse gases generated during cement production, the cost of building materials, and the pressure of waste disposal, showing evident advantages in economic, environmental protection and other aspects. Biomass power plant ash and slag can be applied to setting or added into cement-based composites, displaying a sound micro-aggregate effect [4] and a potential pozzolanic effect [5,6]. However, their complicated role in cement and setting, and unspecified time, effect and mechanism of action result in a biased understanding and use, which, to a certain extent, hinders the application of biomass power plant ash and slag as a resource for building materials. Hence, researching the effect and mechanism of action of biomass power plant ash and slag in cement-based materials is of great guiding significance for the rational use of this resource.

At present, the literature provides some theoretical support for pozzolanic material in eco-friendly cement [7–10], but it has not fully considered the effect of the pozzolanic activity of biomass power plant ash (BPPA) and slag (BPPS) on the structure of P.O and SAC cement mortar [11–13]. There is still great room for improvement regarding the use of biomass power plant ash (BPPA) and slag (BPPS) in P.O and SAC [14–16].

On this basis, in this paper, different dosages of ash and slag from a biomass power plant of the National Bio Energy Group were mixed with Portland cement (P.O) and sulfoaluminate cement (SAC), respectively, to prepare paste samples of the composite cementitious material. The fluidity, setting properties and mechanical properties of the paste samples were tested to evaluate the application performance of the cementitious material in engineering. Moreover, the influences of the ash and slag on the microstructure of hydration minerals of the P.O and SAC paste samples were investigated using characterization methods such as X-ray diffraction (XRD) and scanning electron microscopy (SEM). The research results can provide certain theoretical guidance for the application of biomass power plant ash and slag in cement-based materials.

2. Experiment

2.1. Reagents and Materials

The ash and slag in this experiment came from a biomass power plant of the National Bio Energy Group Ltd, Beijing China. The main fuels of this plant include pine branches and waste wood boards. As found in basic research, the ash and slag from this power plant contain a large amount of CaO, Al_2O_3, SiO_2 and Fe_2O_3, meeting the standards of Class C pozzolanic materials [17,18], and possessing high pozzolanic activity and gelation properties. In addition, the content of CaO and SO_3 in the slag is higher than that in the ash, showing a greater potential for alkali excitation [19]. In this experiment, cyclone separator fly ash (black, dark color and small particle size, as shown in Figure 1a) and boiler bottom slag (taupe, light color, and large particle size with many unburned organic matter, as shown in Figure 1b) were selected. To avoid particle agglomeration, the ash and slag were ground after 3 h of drying in an electric drying oven, and then they were sieved via a 0.25 mm sieve for later use.

Biomass power plant ash (BPPA) and slag (BPPS) were collected from the Ning Yang Biomass Power Plant of the Shandong National Energy Group, China. The chemical and mineralogical compositions of the collected biomass power plant ash and slag were established via X-ray fluorescence (XRF) and X-ray diffraction (XRD) analysis. Table 1 shows the results of the XRF analysis of BPPA and BPPS; the BPPA and BPPS used were mainly composed of SiO_2, Al_2O_3, Fe_2O_3, CaO, and some salts (sulfate and chloride). The X-ray diffraction spectra of BPPA and BPPS (Figure 2) indicated that the minerals in BPPA were dominated by quartz (SiO_2), gypsum ($CaSO_4 \cdot 2H_2O$), calcite ($CaCO_3$), and albite ($Na_2O \cdot Al_2O_3 \cdot 6SiO_2$), among which the peak characteristics of the quartz mineral phase were the most obvious [20–22].

(**a**) (**b**)

Figure 1. Ash and slag of biomass power plant. (**a**) Ash (**b**) slag.

Table 1. Physical and chemical characteristics of BPPA and BPPS.

Parameter	Material (wt%)	
	BPPA	**BPPS**
SiO_2	34.25	44.84
CaO	24.42	11.95
Al_2O_3	5.66	8.08
Fe_2O_3	6.63	6.67
Na_2O	2.00	1.31
MgO	2.01	1.84
K_2O	4.41	6.49
P_2O_5	0.96	1.03
SO_3	10.78	1.92
Cl	2.03	2.59
TiO_2	0.71	1.01
MnO	0.17	0.16
[a] Loss on ignition	6.00	12.12

[a] Loss on ignition at 950 °C.

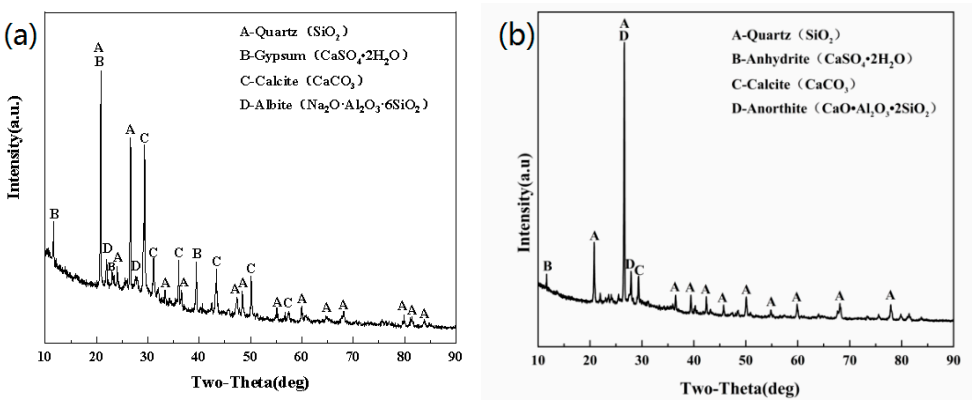

Figure 2. XRD patterns of BPPA (**a**) and BPPS (**b**).

In this experiment, P.O 42.5 produced by Sunnsy Group Jinan, Shandong Province, China and SAC 42.5 produced by China United Cement Co., Ltd, Tangshan, Hebei Province, China were used as the cement materials, the chemical compositions of which are listed in Table 2.

Table 2. Chemical composition of cement (%) a.

Composition	SiO_2	CaO	Al_2O_3	Fe_2O_3	Na_2O	MgO	K_2O	P_2O_5	SO_3	TiO_2	LOI
SAC	9.94	47.47	19.19	3.61	-	1.20	0.32	0.01	16.39	1.36	0.42
P.O	20.68	63.57	4.97	3.76	0.53	2.29	0.8	-	2.00	-	1.4

Note: a data are determined via X-ray fluorescence (XRF) analysis.

2.2. Sample Preparation

The paste samples of the composite cementitious materials were prepared by replacing P.O 42.5 and SAC 42.5 with the biomass power plant ash and slag with different ratios, as shown in Table 3. The OPC and SAC groups, i.e., 100% P.O 42.5 and SAC 42.5 pastes, respectively, were the control groups. Groups OPC-1 to OPC-6 and groups SAC-1 to SAC-6 denote the composite cementitious material samples prepared by adding 10%, 20% and 30% biomass power plant ash and slag, respectively. Other parameters for the OPC and SAC groups were the water/binder ratios of 0.4 and 0.28, and the sample curing times of 1 d, 3 d, 7 d and 28 d, respectively.

Table 3. Paste ratio of composite cementitious materials.

Sample	Cement (wt%)	Ash (wt%)	Slag (wt%)	Water-Binder Ratio
OPC	100	0		0.4
OPC-1	90	10		0.4
OPC-2	80	20		0.4
OPC-3	70	30		0.4
OPC-4	90		10	0.4
OPC-5	80		20	0.4
OPC-6	70		30	0.4
SAC	100	0		0.4
SAC-1	90	10		0.28
SAC-2	80	20		0.28
SAC-3	70	30		0.28
SAC-4	90		10	0.28
SAC-5	80		20	0.28
SAC-6	70		30	0.28

2.3. Testing Method

After 12 h of standard curing, the samples were demolded, transferred into the standard curing box, and taken out for the compressive strength test after the corresponding curing period. Afterward, the internal fragments of the tested samples were selected for XRD and SEM analysis after hydration termination with absolute ethanol.

2.3.1. Fluidity Test

The fluidity of the pastes of the composite cementitious materials made with different ratios was measured using the fluidity tester of cement mortar sand following the Test Method for Fluidity of Cement Mortar (GB/T 2419-2005), and the average of the two results was taken as the measurement result.

2.3.2. Setting Time

An automatic Vicat instrument was used to measure the initial and final setting time of the pastes of composite cementitious materials in accordance with the Test Methods for Water Requirement of Normal Consistency, Setting Time and Soundness of the Portland Cements (GB/T 1346-2011). During the measurement, given the high hydration rate of the SAC clinker and the short setting time, the measurement time was appropriately shortened.

2.3.3. Mechanical Properties

The compressive strength property of the paste samples of the composite cementitious materials was tested in adherence to the Test Method of Cement Mortar Strength (ISO Method) (GB/T 17671-1999). The samples (40 mm × 40 mm × 160 mm cuboids) were tested on a strength testing machine at a loading rate of 2 MPa/s. The average value of the test results of three samples was taken as a representative value, and the relative error was calculated.

2.3.4. XRD Analysis

The internal fragments of the paste samples of the composite cementitious materials cured for 7 d were ground into a powder, sieved, and dried at a low temperature after hydration termination with absolute ethanol. Then, their mineral phases were determined using an X-ray diffractometer under Cu-Kα target radiation, a diffraction angle of 5–80°, and a scanning speed of 5°/min.

2.3.5. SEM Analysis

The paste samples of the composite cementitious materials after 7 d of curing were crushed and ground into a powder, and then dried at a low temperature after hydration termination with absolute ethanol. The morphology of the dried samples was observed under a microscope, and a qualitative analysis of the samples was performed.

2.3.6. Experimental Equipment and Soft Ware

The devices and software that were used to manufacture the composite cementitious materials are shown in Table 4.

Table 4. Experimental equipment and software.

Number	Equipment/Soft Ware	Model	Manufacturer	Country
1	Fluidity tester	NLD-3	Hebei Dahong Experimental Instrument Co., Ltd.	China
2	Automatic pressure measurement testing machine	DYH-300B	ShanDong LuDa Experiment instrument CO., Ltd.	China
3	X-ray fluorescence	D8-advance	USA Thermal Scientific CO., Ltd.	America
4	X-ray diffraction	D/max RB	Rigaku Denki Co., Ltd.	Japan
5	Automatic Vicat instrument	DL-AWK	Daolong Technology Co., Ltd.	China
6	Scanning electron microscopy	Hitachi S2300SEM	Hitachi Co., Ltd.	Japan
7	MDI jade	v6.5	Accelrys Co., Ltd.	America

3. Results and Discussion

3.1. Influence of Ash and Slag Content on the Setting Time of Pastes of Composite Cementitious Materials

According to the influence of biomass ash and slag content on the setting property of the P.O composite cementitious materials shown in Figure 3, the setting time of the composite cementitious material evidently increased with the rising ash and slag content. The control group had an initial and final setting time of 205 min and 258 min, respectively, which were extended to 246 min and 303 min when 30% of the slag was added, and to 242 min and 298 min when 30% of the ash was added, respectively. This reveals that the addition of ash and slag obviously impedes the setting of the pastes of the P.O composite cementitious materials.

The effect of the ash and slag content on the setting property of the SAC composite cementitious materials is shown in Figure 4. As the ash and slag content grew, the setting time of the SAC composite cementitious materials increased, which was still significantly shorter than that of the P.O composite cementitious materials. When the ash and slag content reached 30%, the setting time of the paste of the cementitious material became two times that of the reference paste, increasing from 16 min to 29 min, but still being shorter

than that of the reference P.O 42.5 (242 min). This is because SAC can be quickly hydrated to form ettringite (AFt), leading to fast setting and hardening. Moreover, the crystallization of AFt accelerates the setting of the cementitious material, thereby shortening the setting time.

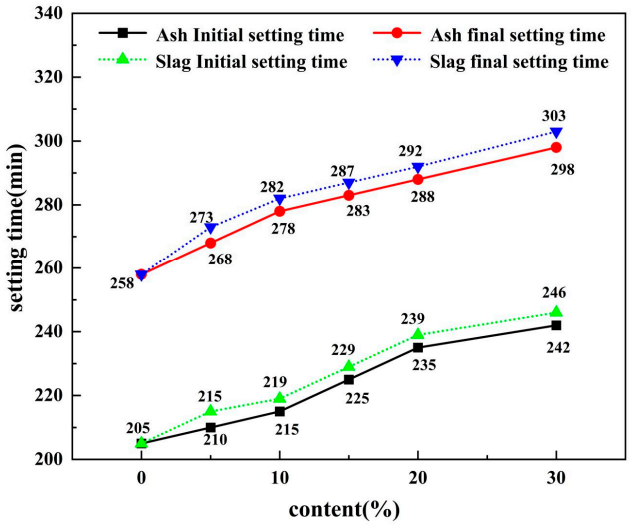

Figure 3. Effect of ash and slag from biomass power plant on setting property of P.O composite cementitious material.

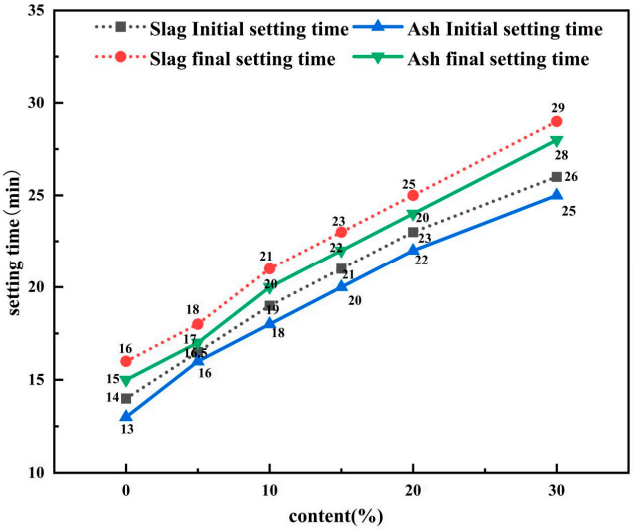

Figure 4. Effect of ash and slag from biomass power plant on setting property of SAC composite cementitious material.

The mechanism of biomass power plant ash and slag hindering the paste setting of the composite cementitious materials involves two aspects. On the one hand, the addition of ash and slag reduces the ratio of cement clinker involved in hydration, thus prolonging the setting of the composite cementitious materials given the much lower hydration activity of ash and slag than that of clinker [23]. On the other hand, the fine particles in ash and slag can fill the gaps between cement particles, thus the setting of cement paste by hindering the contact between cement particles and water molecules. As further observed from the comparison between Figures 2 and 3, the content of biomass power plant slag had a larger impact on the setting time of the composite cementitious materials than that of ash, indicating that it prolongs the setting time more effectively. This can be explained by the fact that the soluble sulfate in the ash and slag reacts with the calcium aluminate in the cement to form a sulfoaluminate coating on the surface of the cement particles, thus causing the reduced hydration activity of the cement particles and the delayed hydration

reaction of the cement clinker [24,25]. The higher soluble sulfate content in slag compared to that of ash brings a stronger ability to impede the setting of cementitious materials.

3.2. Influence of the Ash and Slag Content on the Fluidity of the Pastes of Composite Cementitious Materials

The effect of the biomass power plant ash and slag content on the fluidity of the composite cementitious materials is provided in Figure 5. In the absence of ash and slag content, the maximum fluidities of the P.O and SAC composite cementitious materials were 18.33 cm and 18.6 cm, respectively, which were significantly improved after the addition of ash and slag. Under the same content, the biomass power plant ash and slag exhibited a better improvement effect on the fluidity of the P.O composite cementitious materials than on the SAC composite cementitious materials. When the ash and slag content was 30%, the maximum fluidity of the P.O and SAC composite cementitious materials increased to 26.7 cm (45.6%) and 22 cm (18.2%), respectively. Ash and slag can improve the gradation of the cement pastes [26], fill the gaps between cement particles, promote the gradation between cementitious material particles, and lower the yield stress and apparent viscosity of pastes, thereby increasing the fluidity [27].

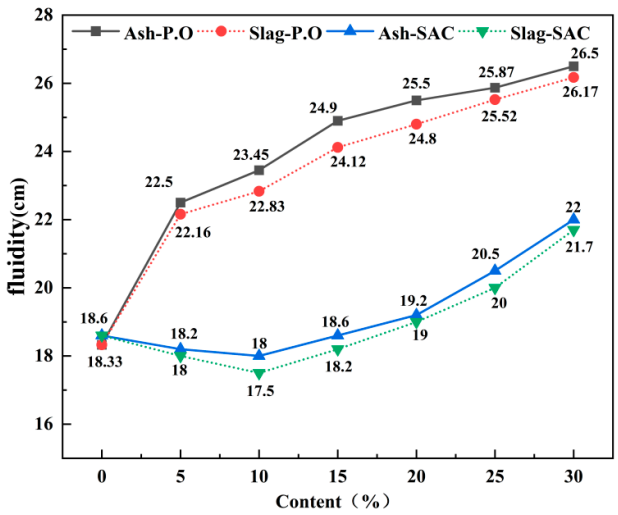

Figure 5. Effect of ash/slag content of biomass power plant on fluidity of composite cementitious material.

The fluidity of the pastes of the SAC composite cementitious materials experienced a decreasing-then-increasing trend, decreasing to 18.0 cm and 17.5 cm, respectively, as the ash and slag content increased to 10%, and increasing to 21.7 cm and 22.0 cm, respectively, as the content continued to increase to 30%. This can be attributed to the irregular shapes and rough surfaces of the ash and slag. At a low ash and slag content, the friction between the pastes is increased, thus hindering the flow of pastes [28]. The porous structure of unburned organic matter enables it to absorb a certain amount of free water [29], further reducing the fluidity of pastes. However, as the ash and slag content rises, the gradation improvement effect of ash and slag gradually plays a dominant role, contributing to the flow of pastes and hence improving the fluidity.

The fluidity of the pastes of the SAC composite cementitious materials underwent a decreasing-then-increasing trend, specifically, decreasing to 18.0 cm and 17.5 cm, respectively, as the ash and slag content increased to 10%, and increasing to 21.7 cm and 22.0 cm, respectively, as the content continually increased to 30%. This can be attributed to the irregular shape and the many cluster structures of the biomass power plant ash and slag, resulting in rough surfaces. This enlarges the friction between pastes at the low ash and slag content [30]. Moreover, the unburned organic matters contained in the ash and slag also reduced the fluidity of the paste slag, since they have a porous structure and can absorb

a certain amount of free water [31]. The fluidity increased as the ash and slag content rose, mostly due to the appropriate gradation promoting the flow of pastes.

3.3. Influence of Ash and Slag Content on the Mechanical Properties of Composite Cementitious Materials

The compressive strength test results of the hardened pastes of the composite cementitious materials prepared using the biomass power plant ash and slag are displayed in Figures 6 and 7. Compared with the controls, the composite cementitious materials experienced a downward trend at each curing time with the rising ash and slag content, and an upward trend with the growing curing time. At the curing time of 1 d, the compressive strength of the pastes of the controls reached 20.3 MPa (P.O) and 56.0 MPa (SAC), 16.7% and 16.0% higher than that (16.9 MPa and 17.05 MPa) of the P.O composite cementitious materials at the 10% ash and slag content, and 21.4% and 17.0% higher than that (44.0 MPa and 46.5 MPa) of the SAC composite cementitious materials at the 10% ash and slag content. The main reason is that the addition of ash and slag lowers the ratio of cement clinker, and the biomass power plant ash and slag are subjected to poor activity in the early stage and a low degree of hydration, causing the strength of the composite cementitious material sample to decrease with the growing ash and slag content in the early stage.

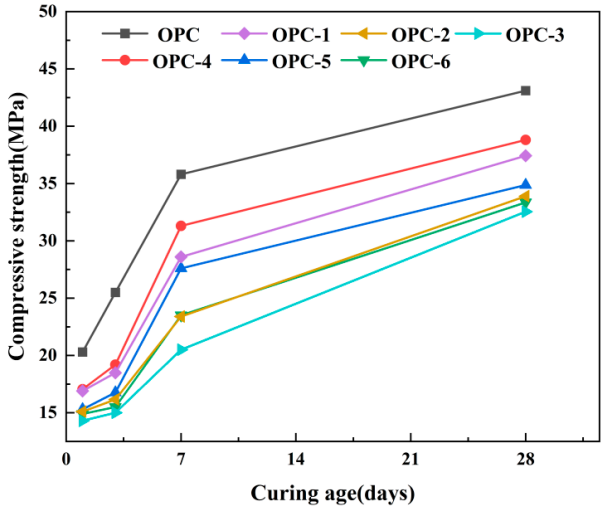

Figure 6. Effect of ash/slag content of biomass power plant on compressive strength property of P.O composite cementitious material.

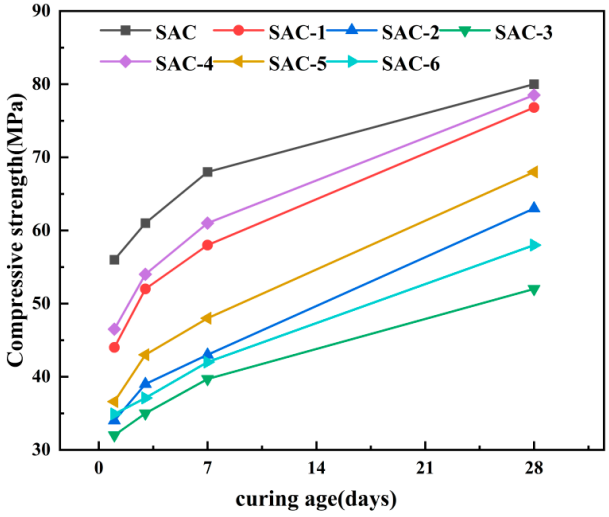

Figure 7. Effect of ash/slag content of biomass power plant on compressive strength of SAC composite cementitious material.

As the curing time increased, the compressive strength of the pastes of the composite cementitious materials began to increase gradually, showing a gradually narrowing difference between it and the controls. At the curing time of 28 d, the compressive strengths of the P.O composite cementitious material samples with 10% ash and slag were 42.8 MPa and 40.43 MPa, respectively, only 0.7% and 6.2% lower than that of the control group, and the compressive strength of the SAC composite cementitious material made with 10% ash and slag were 76.8 MPa and 78.5 MPa, respectively, only 4.0% and 2.0% lower than that of the control group. This is because the pozzolanic activity of the biomass power plant ash and slag is stimulated as the hydration reaction proceeds, and hydration products such as calcium silicate hydrate (C-S-H) and calcium aluminate hydrate (C-A-H) further compact the pastes and improve their mechanical strength [32], resulting in a rapid increase in the compressive strength of the composite cementitious materials. However, the compressive strength of the hardened pastes of the composite cementitious materials underwent a large decrease as the ash and slag content increased to 30%. At the age of 28 d, the compressive strengths of the hardened pastes of the SAC composite cementitious materials were 41.3% and 30.0% lower than those of the control group, respectively, and the compressive strengths of the hardened pastes of the P.O composite cementitious materials were 22.6% and 24.5% lower than those of the control group, respectively. The reason for this is that, at the high ash and slag content, the ratio of cement clinker is greatly reduced and the hydration reaction of cement clinker plays a dominant role in the hydration of the composite cementitious materials, leading to an evident decrease in the compressive strength of the pastes of the composite cementitious materials. Hence, for the good compressive strength of the composite cementitious materials, the ash and slag content should be no larger than 20%.

3.4. Influence of Ash and Slag on the Hydration Minerals in the Composite Cementitious Material System

The XRD patterns of the hydration products of the P.O composite cementitious materials prepared by adding biomass power plant ash and slag after 7 d of hydration are provided in Figures 8 and 9. It can be found that the types of hydration products were not affected by the addition of ash and slag in P.O, and remained to be AFt, calcium hydroxide (CH), semicarbohydrate aluminum carbonic acid [$Ca_4Al_2O_6(CO_3)_{0.5}(OH)\cdot 11.5H_2O$], dicalcium silicate ($C_2S$), calcium carbonate ($CaCO_3$) and quartz ($SiO_2$), without the generation of new hydration products. CH is formed by the hydration of tricalcium silicate (C_3S) and C_2S clinker in the P.O composite cementitious materials (Formulas (1) and (2)) [33]. C-S-H belongs to the amorphous phase, which cannot be directly characterized in XRD patterns. In addition, AFt is the product of the reaction of C-A-H [generated by clinker hydration of tricalcium aluminate (C_3A) and tetracalcium aluminoferrate (C_4AF) (Formulas (3) and (4))] with gypsum ($CaSO_4\cdot 2H_2O$) (Formula (5)) [34]. The weak diffraction peaks of $CaCO_3$ and $Ca_4Al_2O_6(CO_3)_{0.5}(OH)\cdot 11.5H_2O$ in the XRD patterns may be related to the carbonization reaction during sampling, sample preparation or testing. The diffraction peak of C_2S in the patterns may come from the slow hydration of some C_2S [35]. After 7 d of curing, some C_2S was not fully hydrated.

$$2(3CaO\cdot SiO_2) + 6H_2O = 3CaO\cdot 2SiO_2\cdot 3H_2O + 3Ca(OH)_2 \quad (1)$$

$$2(2CaO\cdot SiO_2) + 4H_2O = 3CaO\cdot 2SiO_2\cdot 3H_2O + Ca(OH)_2 \quad (2)$$

$$3CaO\cdot Al_2O_3 + 6H_2O = 3CaO\cdot Al_2O_3\cdot 6H_2O \quad (3)$$

$$4CaO\cdot Al_2O_3\cdot Fe_2O_3 + 7H_2O = 3CaO\cdot Al_2O_3\cdot 6H_2O + CaO\cdot Fe_2O_3\cdot H_2O \quad (4)$$

$$3CaO\cdot Al_2O_3\cdot 6H_2O + 3(CaSO_4\cdot 2H_2O) + 19H_2O = 3CaO\cdot Al_2O_3\cdot 3CaSO_4\cdot 31H_2O \quad (5)$$

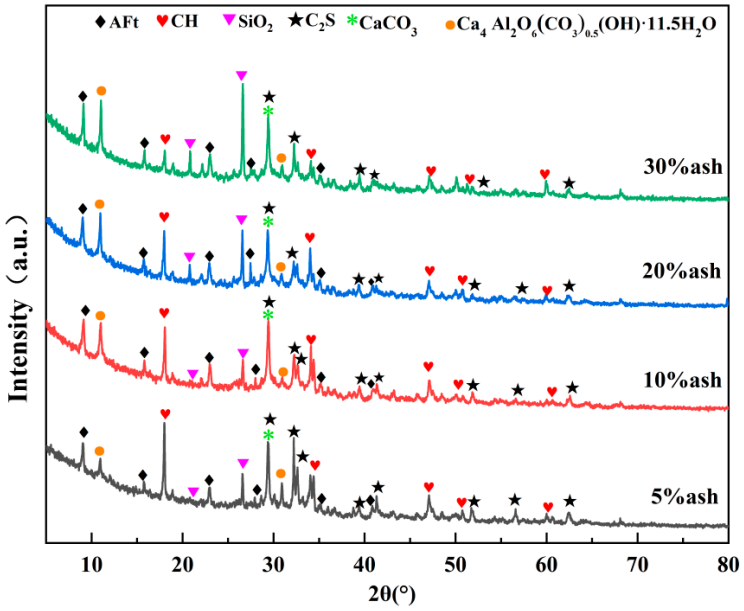

Figure 8. X-ray diffraction pattern of hydration product of ash–P.O composite cementitious material of biomass power plant for 7 days.

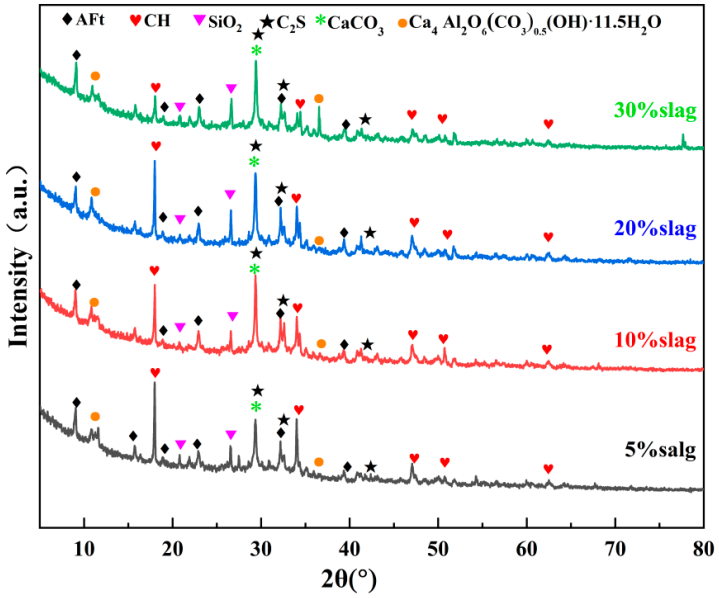

Figure 9. X-ray diffraction pattern of 7-day hydration product of biomass power plant slag–P.O composite cementitious material.

As Figure 10 shows, the characteristic peaks of CH in the hydration products were gradually less intensive with the rising ash and slag content. This is because CH can react with the active SiO_2 and Al_2O_3 in ash and slag to generate C-S-H and C-A-H, thus consuming part of CH [36] and eventually causing a decrease in the CH diffraction peaks and promoting the hydration of P.O clinker [37].

$$3SiO_2 + xCa(OH)_2 + (n - x)H_2O = xCaO{\cdot}SiO_2{\cdot}nH_2O \quad (6)$$

$$3Al_2O_3 + xCa(OH)_2 + (n - x)H_2O = xCaO{\cdot}Al_2O_3{\cdot}nH_2O \quad (7)$$

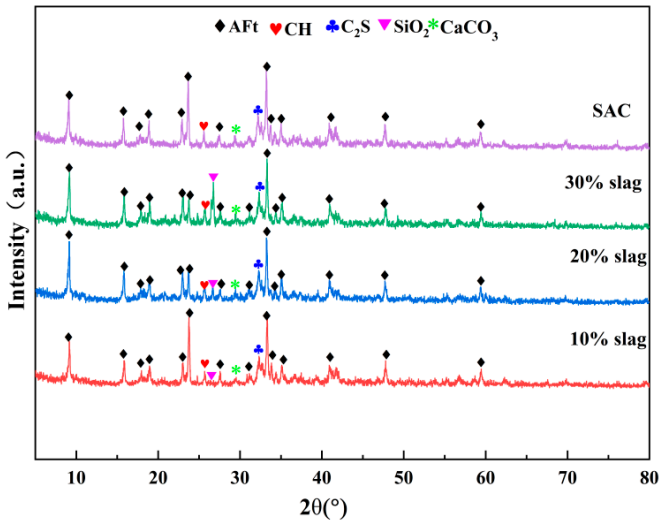

Figure 10. X-ray diffraction pattern of hydration product of biomass power plant slag SAC composite.

The XRD patterns of the SAC composite cementitious materials after 7 d of hydration are shown in Figures 10 and 11. AFt, C_2S, $CaCO_3$, CH and SiO_2 were found to be the main hydration minerals of the SAC composite cementitious materials made with ash and slag. Among them, AFt has the strongest and most widely distributed diffraction peaks, and it provides early strength. AFt, CH, and alumina trihydrate (AH_3) are the products of the rapid hydration of anhydrous calcium sulfoaluminate and C_2S in the SAC composite cementitious materials [38,39]. The AH_3 and C-S-H gel among the hydration products cannot be characterized in the XRD patterns due to the poor crystallization. As further found from Figure 11, with the 10% biomass power plant slag, the peak of the SiO_2 in the hydration sample of the composite cementitious materials was less intensive. The reason for this is that a pozzolanic reaction occurs between the SiO_2 in the biomass power plant slag and CH in the hydration system [40], thus consuming part of the SiO_2.

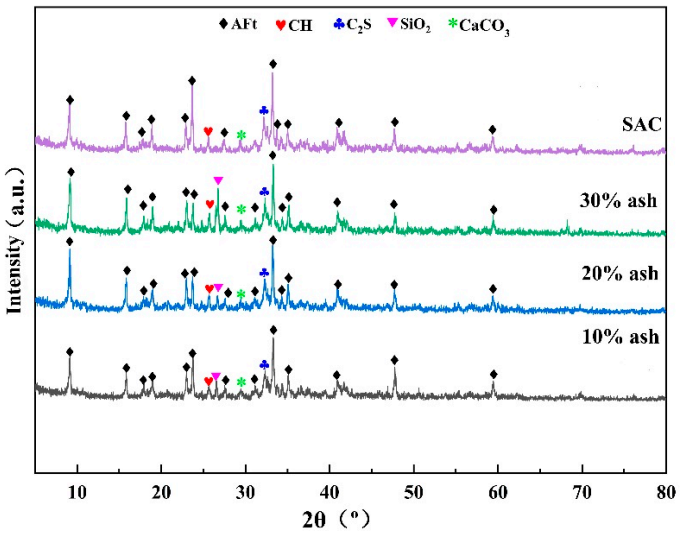

Figure 11. X-ray diffraction pattern of the hydration product of the ash SAC composite cementitious material from the biomass power plant for 7 days.

3.5. Influence of Ash and Slag on the Microstructure of Hydration Minerals in the Composite Cementitious Material System

The SEM images of the P.O composite cementitious materials made with biomass power plant ash and slag after 7 d of hydration are shown in Figure 12. A large number

of hydration products, such as sheet-like CH, flocculent C-S-H gel, and needle–rod-like Aft, were found to be formed at 7 d of hydration of the composite cementitious materials, in line with the XRD analysis results. The C-S-H gel can fill the voids of the AFt network structure, connect the hydration products, compact the microstructure of the hardened pastes of the cementitious materials, and boost the strength development of the hardened pastes. Moreover, according to Figure 12, only a small amount of sheet-like CH phase exists, and CH is the main hydration product of P.O composite cementitious materials. The reason is that the consumption of CH in the pozzolanic reaction of ash and slag results in a reduction in sheet-like CH in the microstructure of hydration products [41].

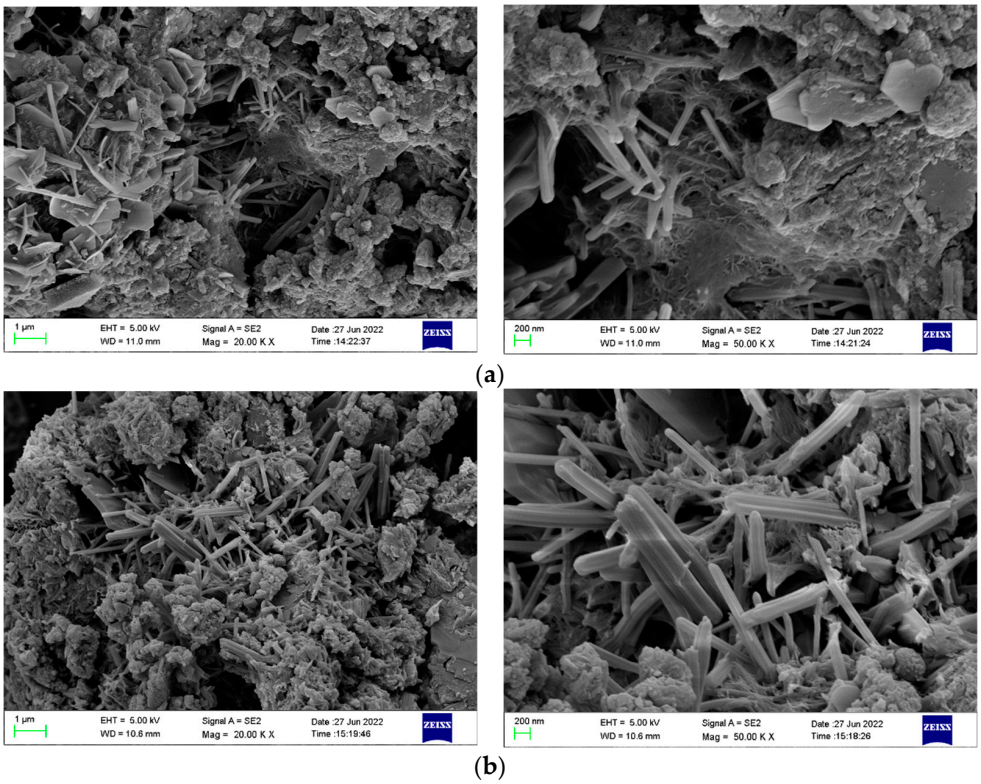

Figure 12. SEM images of 7 d hydration sample of P.O composite cementitious material. (**a**) P.O composite cementitious material made with 10% biomass power plant ash. (**b**) P.O composite cementitious material made with 10% biomass power plant slag.

The SEM images of the SAC composite cementitious materials made with different contents of biomass power plant ash and slag after 7 d of hydration are shown in Figure 13. After 7 d of hydration, abundant hydration products were found to be produced in the SAC composite cementitious materials and a large number of intersecting needle–rod-like AFt and flocculent (AH_3 and C-S-H) structures were also observed. The rapid hydration of the SAC clinker can form rich needle–rod-like AFt, intersecting to form a network structure. AH3 and C-S-H fill the network, compact the paste structure, and quickly form the strength in the early stage, resulting in the obvious higher strength of the SAC composite cementitious materials in the early stage compared to that of the P.O composite cementitious materials. As the hydration proceeds, the active Al_2O_3 and SiO_2 in the biomass power plant ash and slag are stimulated by the alkaline environment formed by SAC hydration to undergo pozzolanic reactions, thus producing gels such as C-S-H and C-A-H, and filling the network structure of AFt [42,43]. This makes the pastes more compact, accelerating the development of the strength of the SAC composite cementitious material in the late stage. According to the comparison of the SEM images of the samples in Figure 12 after 7 d of hydration, the composite cementitious material made with a small amount of biomass power plant slag is more compact, has a higher degree of hydration,

has more uniform hydration products, and has less obvious particle interfaces. Moreover, it is firmly connected to the surrounding gel products as a whole and shows the compact structure of the hardened pastes. Hence, the strength of the SAC composite cementitious materials made with biomass power plant slag is better.

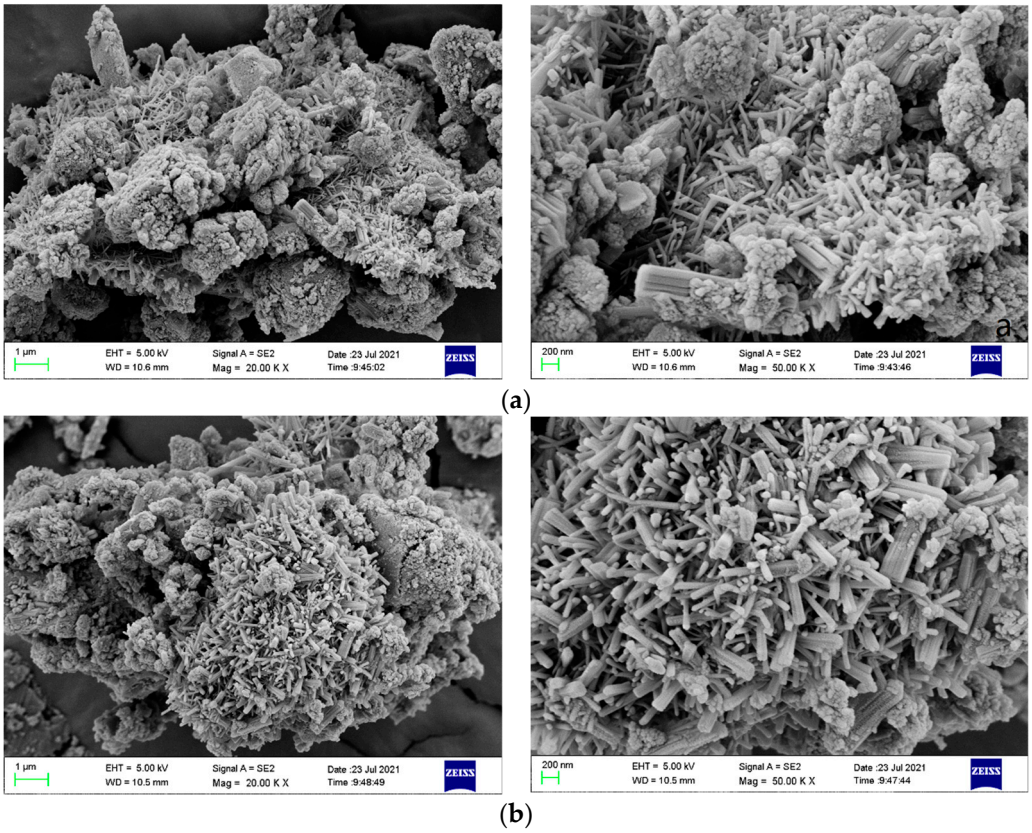

Figure 13. SEM images of 7 d hydration sample of SAC composite cementitious material. (**a**) P.O composite cementitious material made with 10% biomass power plant ash. (**b**) P.O composite cementitious material made with 10% biomass power plant slag.

4. Conclusions

(1) The compressive strength of the P.O and SAC pastes gradually decreased with the rising ash and slag content. Compared with the reference cement, the 28 d compressive strength of the P.O pastes made with 30% biomass power plant ash and slag decreased by 27.8% and 15.0%, respectively, while that of the SAC pastes decreased by 27.5% and 35.0%, respectively. Nonetheless, the increase in the compressive strength was faster at the curing time of 7 d to 28 d, close to that of the control groups.

(2) The addition of biomass power plant ash and slag could significantly prolong the setting time of P.O and SAC pastes, and the setting hindrance effect was more significant with the rising content. Using the 50% biomass power plant slag, the initial and final setting time of the P.O pastes grew by 28.8% and 25.2%, respectively, and that of the SAC pastes both grew by 50%.

(3) After the addition of the biomass power plant ash and slag, the fluidity of the P.O and SAC pastes showed an upward trend and a decreasing-then-increasing trend as the ash and slag content increased, respectively.

(4) According to the phase and microscopic analysis, the hydration of the P.O pastes was promoted after the addition of biomass power plant ash and slag, and the CH peaks in the products after 7 d of hydration were less intensive. The addition of ash and slag also promoted the clinker hydration of SAC pastes, resulting in an obvious increase in the AFt among the 7 d hydration products and a compact structure.

Author Contributions: Methodology, Y.Z.; resources, B.Z.; funding acquisition, J.Z.; data curation, Z.W.; writing—original draft preparation, C.R.; writing—review and editing, H.X.; formal analysis, H.G.; D.Z., supervision. All authors have read and agreed to the published version of the manuscript.

Funding: This research received no external funding.

Data Availability Statement: The research data is unavailable due to privacy and ethical restrictions.

Acknowledgments: The authors express their heartfelt gratitude to the National Energy Biomass Power Generation Group Co., Ltd. science and technology project 'SGTYHT/20-JS-221'.

Conflicts of Interest: The authors declare no conflict of interest.

References

1. Shi, Y.; Xue, C.; Qiu, Y.P. Analysis and Prospect of ash recycling technology in agricultural and forestry biomass direct fired power plants. *J. Agric. Resour. Environ.* **2019**, *2*, 13–17.
2. Ren, C.Z.; Wang, W.L.; Mao, Y.P.; Yuan, Y.P.; Song, Z.L.; Sun, J.; Zhao, X.Q. Comparative life cycle assessment of sulfoaluminate clinker production derived from industrial solid wastes and conventional raw materials. *J. Clean. Prod.* **2017**, *167*, 1314–1324. [CrossRef]
3. Zhou, N.; Fridley, D.; Khanna, N.Z.; Ke, J.; McNeil, M.; Levine, M. China's energy and emissions outlook to 2050: Perspectives from bottom-up energy end-use model. *Energy Policy* **2013**, *53*, 51–62. [CrossRef]
4. Shuai, C.Y.; Chen, X.; Wu, Y.; Zhang, Y.; Tan, Y. A three-step strategy for decoupling economic growth from carbon emission: Empirical evidences from 133 countries. *Sci. Total Environ.* **2018**, *646*, 524–543. [CrossRef] [PubMed]
5. Demis, S.; Tapali, J.G.; Papadakis, V.G. An investigation of the effectiveness of the utilization of biomass ashes as pozzolanic materials. *Constr. Build. Mater.* **2014**, *68*, 291–300. [CrossRef]
6. Raheem, A.A.; Adenuga, O.A. Wood Ash from Bread Bakery as Partial Replacement for Cement in Concrete. *Int. J. Sustain. Constr. Eng. Technol.* **2013**, *4*, 75–81.
7. Nehring, V.; Silva, L.H.P.; de Maria, P.K.V.; de Paiva, F.F.G.; Tamashiro, J.R.; dos Santos, L.F.; Teixeira, S.R.; Kinoshita, A. Recycling of bamboo leaves and use as pozzolanic material to mitigate degradation of cementitious composites. *Clean. Waste Syst.* **2022**, *3*, 100053. [CrossRef]
8. Zheng, X.; Liu, K.F.; Gao, S.Z.; Wang, F.Z.; Wu, Z.Z. Effect of pozzolanic reaction of zeolite on its internal curing performance in cement-based materials. *J. Build. Eng.* **2023**, *63*, 105503. [CrossRef]
9. Georgopoulos, G.; Aspiotis, K.; Badogiannis, E.; Tsivilis, S.; Perraki, M. Influence of mineralogy and calcination temperature on the behavior of palygorskite clay as a pozzolanic supplementary cementitious material. *Appl. Clay Sci.* **2023**, *232*, 106797. [CrossRef]
10. Swathi, V.; Asadi, S.S. An influence of pozzolanic materials with hybrid fibers on structural performance of concrete: A review. *Mater. Proc.* **2021**, *43*, 1956–1959. [CrossRef]
11. Wang, H.Y.; Tsai, S.L.; Hung, C.C.; Jian, T.Y. Research on engineering properties of cement mortar adding stainless steel reduction slag and pozzolanic materials. *Case Stud. Constr. Mater.* **2022**, *16*, 1144. [CrossRef]
12. Berenguer, R.; Lima, N.; Pinto, L.; Monteiro, E.; Povoas, Y.; Oliveira, R. Cement-based materials: Pozzolanic activities of mineral additions are compromised by the presence of reactive oxides. *J. Build. Eng.* **2021**, *41*, 102358. [CrossRef]
13. Cheng, S.K.; Ge, K.Y.; Sun, T.; Shui, Z.H.; Chen, X.Y.; Lu, J.-X. Pozzolanic activity of mechanochemically and thermally activated coal-series kaolin in cement-based materials. *Constr. Build. Mater.* **2021**, *299*, 123972. [CrossRef]
14. Kapeluszna, E.; Kotwica, Ł.; Malata, G.; Murzyn, P.; Nocuń-Wczelik, W. The effect of highly reactive pozzolanic material on the early hydration of alite—C_3A—Gypsum synthetic cement systems. *Constr. Build. Mater.* **2020**, *251*, 118879. [CrossRef]
15. da Silva, A.R.; de Paiva, F.F.G.; Silva, L.H.P.; dos Santos, L.F.; Tolosa, G.R.; Job, A.E.; Galvín, A.P.; López-Uceda, A.; Teixeira, S.R.; Kinoshita, A.; et al. Evaluation of pozzolanic activity and environmental assessment of cement composites with lubricating oil re-refining ash. *Constr. Build. Mater.* **2023**, *376*, 130980. [CrossRef]
16. Zhang, H.R.; Ji, T.; Liu, H.; Su, S.L. Improving the sulfate resistance of recycled aggregate concrete (RAC) by using surface-treated aggregate with sulfoaluminate cement (SAC). *Constr. Build. Mater.* **2021**, *297*, 123535. [CrossRef]
17. Xie, H.Z.; Ren, C.Z.; Zhao, B.F.; Liu, S.X.; Zhu, D.; Guan, H.B.; Xu, D.; Wang, J.W.; Yang, H.J. Characterization and use of biomass power plant ash in sulfoaluminate cementitious materials. *Constr. Build. Mater.* **2022**, *325*, 126667. [CrossRef]
18. Olafusi, O.S.; Kupolati, W.K.; Sadiku, R.; Snyman, J.; Ndambuki, J.M. Characterization of corncob ash (CCA) as a pozzolanic material. *Int. J. Civ. Eng. Technol.* **2018**, *9*, 1016.
19. Chen, R.; Congress, S.S.C.; Cai, G.; Duan, W.; Liu, S. Sustainable utilization of biomass waste-rice husk ash as a new solidified material of soil in geotechnical engineering: A review. *Constr. Build. Mater.* **2021**, *292*, 123219. [CrossRef]
20. Kolesnikova, O.; Syrlybekkyzy, S.; Fediuk, R.; Yerzhanov, A.; Nadirov, R.; Utelbayeva, A.; Agabekova, A.; Latypova, M.; Chepelyan, L.; Volokitina, I.; et al. Thermodynamic Simulation of Environmental and Population Protection by Utilization of Technogenic Tailings of Enrichment. *Materials* **2022**, *15*, 6980. [CrossRef]

21. Zhanikulov, N.N.; Khudyakova, T.M.; Taimasov, B.T.; Sarsenbayev, B.K.; Dauletiarov, M.S.; Kolesnikov, A.S.; Karshygayev, R.O. Receiving Portland Cement from Technogenic Raw Materials of South Kazakhstan. *Eurasian Chem. Technol. J.* **2019**, *21*, 333–340. [CrossRef]
22. Kolesnikova, O.; Vasilyeva, N.; Kolesnikov, A.; Zolkin, A. Optimization of raw mix using technogenic waste to produce cement clinker. *MIAB Min. Inf. Anal. Bull.* **2022**, *10*, 103–115. [CrossRef]
23. Ukrainczyk, N.; Vrbos, N.; Koenders, E.A.B. Reuse of woody biomass ash waste in cementitious materials. *Chem. Biochem. Eng. Q.* **2016**, *30*, 137–148. [CrossRef]
24. da Silva Andrade Neto, J.; De la Torre, A.G.; Kirchheim, A.P. Effects of sulfates on the hydration of Portland cement—A review. *Constr. Build. Mater.* **2021**, *279*, 122428. [CrossRef]
25. Lv, Q.F.; Wang, Z.S.; Gu, L.Y.; Chen, Y.; Shan, X.K. Effect of sodium sulfate on strength and microstructure of alkali-activated fly ash based geopolymer. *J. Cent. South Univ.* **2020**, *27*, 1691–1702. [CrossRef]
26. Bonfim, W.B.; de Paula, H.M. Characterization of different biomass ashes as supplementary cementitious material to produce coating mortar. *J. Clean. Prod.* **2021**, *291*, 125869. [CrossRef]
27. Hu, J.; Wang, K. Effect of coarse aggregate characteristics on concrete rheology. *Constr. Build. Mater.* **2011**, *25*, 1196–1204. [CrossRef]
28. Feys, D.; Verhoeven, R.; Schutter, G.D. Why is fresh self-compacting concrete shear thickening? *Cem. Concr. Res.* **2009**, *39*, 510–523. [CrossRef]
29. Thomas, B.S.; Yang, J.; Mo, K.H.; Abdalla, J.A.; Hawileh, R.A.; Ariyachandra, E. Biomass ashes from agricultural wastes as supplementary cementitious materials or aggregate replacement in cement/geopolymer concrete: A comprehensive review. *J. Build. Eng.* **2021**, *10*, 2332. [CrossRef]
30. Yang, Z.; Huddleston, J.; Brown, H. Effects of wood ash on properties of concrete and flowable fill. *J. Mater. Sci. Chem. Eng.* **2016**, *4*, 101–114. [CrossRef]
31. Ayub, M.; Othman, M.H.D.; Khan, I.U.; Hubadillah, S.K.; Kurniawan, T.A.; Ismail, A.F.; Rahman, M.A.; Jaafar, J. Promoting sustainable cleaner production paradigms in palm oil fuel ash as an eco-friendly cementitious material: A critical analysis. *J. Clean. Prod.* **2021**, *295*, 126296. [CrossRef]
32. Hou, G.H.; Shen, X.D.; Xu, Z.Z. Study on the composition and properties of high silicate tricalcium Portland cement clinker. *Acta Silic. Sin.* **2014**, *32*, 5–10.
33. Fang, P. A study of applying basic oxygen furnace slag to cement grouting repairing or strengthening material. *Cem. Concr. Compos.* **2015**, *22*, 12–25.
34. Ye, Z.Y.; Wang, Q.Q. Preparation and properties of aluminosilicate solid waste cementitious material. *Gold Sci. Technol.* **2020**, *28*, 658–668.
35. Zhu, J.; Yang, K.; Chen, Y.; Fan, G.; Zhang, L.; Guo, B.; Guan, X.; Zhao, R. Revealing the substitution preference of zinc in ordinary Portland cement clinker phases: A study from experiments and DFT calculations. *J. Hazard. Mater.* **2021**, *409*, 124504. [CrossRef]
36. Zheng, K.R.; Chen, L.; Zhou, J. Pozzolanic reaction of glass powder and its influence on the composition of hydrated calcium silicate. *Acta Silic. Sin.* **2016**, *44*, 202–210.
37. Wang, H.; Zhang, A.-l.; Zhang, L.-c.; Wang, Q.; Han, Y.; Liu, J.-z.; Gao, X.-j.; Shi, F.-t.; Lin, X.-y.; Feng, L.-y. Hydration process of rice husk ash cement paste and its corrosion resistance of embedded steel bar. *J. Cent. South Univ.* **2020**, *27*, 3464–3476. [CrossRef]
38. Yao, Y.; Wang, W.; Ge, Z.; Ren, C.; Yao, X.; Wu, S. Hydration study and characteristic analysis of a sulfoaluminate high-performance cementitious material made with industrial solid wastes. *Cem. Concr. Compos.* **2020**, *112*, 103687. [CrossRef]
39. Wu, K.; Shi, H.; Guo, X. Utilization of municipal solid waste incineration fly ash for sulfoaluminate cement clinker production. *Waste Manag.* **2011**, *31*, 2001–2008. [CrossRef]
40. Wang, S. Quantitative kinetics of pozzolanic reactions in coal/cofired biomass fly ashes and calcium hydroxide (CH) mortars. *Constr. Build. Mater.* **2014**, *51*, 364–371. [CrossRef]
41. Rashad, A.M. Investigation on high-volume fly ash pastes modified with micro-size metakaolin subjected to high temperatures. *J. Cent. South Univ.* **2020**, *27*, 231–241. [CrossRef]
42. Kolesnikov, A.S.; Sapargaliyeva, B.O.; Bychkov, A.Y.; Alferyeva, Y.O.; Syrlybekkyzy, S.; Altybaeva, Z.K.; Nurshakhanova, L.K.; Seidaliyeva, L.K.; Suleimenova, B.S.; Zhidebayeva, A.E.; et al. Thermodynamic modeling of the formation of the main minerals of cement clinker and zinc fumes in the processing of toxic technogenic waste of the metallurgical industry. *Rasayan J. Chem.* **2022**, *15*, 2181–2187. [CrossRef]
43. Taimasov, B.T.; Sarsenbayev, B.K.; Khudyakova, T.M.; Kolesnikov, A.S.; Zhanikulov, N.N. Development and testing of low-energy intensive technology of receiving sulfate-resistant and road Portland cement. *Eurasian Chem. Technol. J.* **2017**, *19*, 347–355. [CrossRef]